

# Selective C-Terminal Conjugation of Protease-Derived Native Peptides for Proteomic Measurements

Tian Xie, Alexandria Brady, Cecilia Velarde, David N. Vaccarello, Nicholas W. Callahan, John P. Marino, and Sara V. Orski\*



Cite This: *Langmuir* 2022, 38, 9119–9128



Read Online

ACCESS |



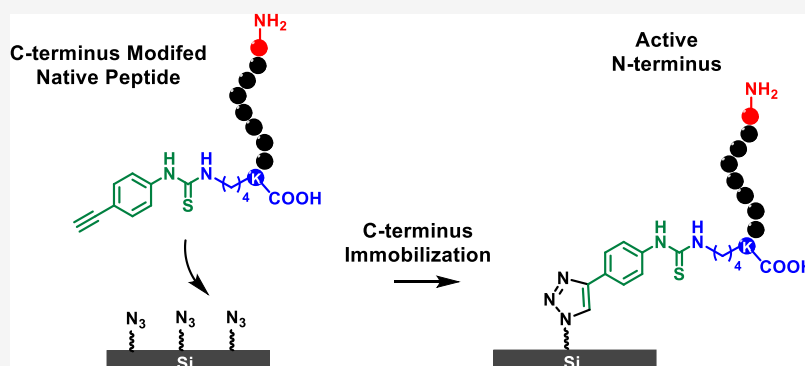
Metrics & More



Article Recommendations



Supporting Information



**ABSTRACT:** Bottom-up proteomic experiments often require selective conjugation or labeling of the N- and/or C-termini of peptides resulting from proteolytic digestion. For example, techniques based on surface fluorescence imaging are emerging as a promising route to high-throughput protein sequencing but require the generation of peptide surface arrays immobilized through single C-terminal point attachment while leaving the N-terminus free. While several robust approaches are available for selective N-terminal conjugation, it has proven to be much more challenging to implement methods for selective labeling or conjugation of the C-termini that can discriminate between the C-terminal carboxyl group and other carboxyl groups on aspartate and glutamate residues. Further, many approaches based on conjugation through amide bond formation require protection of the N-terminus to avoid unwanted cross-linking reactions. To overcome these challenges, herein, we describe a new strategy for single-point selective immobilization of peptides generated by protease digestion via the C-terminus. The method involves immobilization of peptides via lysine amino acids which are found naturally at the C-terminal end of cleaved peptides from digestions of certain serine endoproteases, like LysC. This lysine and the N-terminus, the sole two primary amines in the peptide fragments, are chemically reacted with a custom phenyl isothiocyanate (EPITC) that contains an alkyne handle. Subsequent exposure of the double-modified peptides to acid selectively cleaves the N-terminal amino acid, while the modified C-terminus lysine remains unchanged. The alkyne-modified peptides with free N-termini can then be immobilized on an azide surface through standard click chemistry. Using this general approach, surface functionalization is demonstrated using a combination of X-ray photoelectron spectroscopy (XPS), ellipsometry, and atomic force microscopy (AFM).

## 1. INTRODUCTION

The controlled immobilization of biomolecules such as proteins and oligonucleotides on material surfaces is critical in biological research, as it underpins the advancement of various biotechnologies such as microarrays,<sup>1,2</sup> biosensing,<sup>3</sup> drug delivery,<sup>3,4</sup> and tissue engineering.<sup>5</sup> Microarrays are particularly useful in bioanalytical research since they allow highly parallel, multiplex analysis of biomolecules in a rapid and miniaturized manner. For example, DNA microarrays were developed three decades ago based on the hybridization between complementary DNA strands from the surface-immobilized features and the fluorophore-labeled sample. These arrays have become a standard tool for genome

interpretation and have been broadly applied in genomic research and diagnostic applications.<sup>6–8</sup> Peptide microarrays have also been studied extensively and have found applications in diagnostics, ligand binding, cell adhesion, and biosensing.<sup>9,10</sup> Recently, a growing effort has been put into developing massively parallel protein sequencing platforms that are akin to

**Received:** February 11, 2022

**Revised:** April 29, 2022

**Published:** July 20, 2022



what has been developed for next-generation DNA sequencing.<sup>11</sup> A peptide microarray-based protein sequencing platform would allow direct, parallel measurement of the amino acid (AA) sequences from surface-immobilized peptides with higher throughput, sensitivity, and dynamic range.<sup>12,13</sup> When developing peptide microarrays for peptide sequencing applications, some methods require the use of Edman degradation on the N-termini of immobilized peptides to repetitively remove the terminal AA, and thus expose the next AA in sequence to allow for sequential AA identification. Therefore, having active N-termini on the immobilized peptides is crucial for these applications. Peptide surface arrays immobilized with functional N-termini can also be beneficial for peptide functionalization research involving N-terminal acetylation, acylation, and transamination reactions.<sup>14</sup>

Currently, numerous strategies are available to tether proteins to surfaces. One of the most common approaches involves covalent bonding through conjugation of the natural functionality of specific amino acid residues with a functionalized surface. Examples include the reaction between lysine and an *n*-hydroxysuccinimide (NHS)-ester<sup>15</sup> or aldehyde surface<sup>16,17</sup> or a thiol–ene click reaction between cysteine and a maleimide surface.<sup>18,19</sup> Although these methods are highly successful at immobilizing proteins and peptides, they can create several points of attachment in the process due to the multiple copies of each reactive residue in the protein. A number of approaches are also described for point selective conjugation and labeling through the N-terminal amine.<sup>20</sup> Another common immobilization strategy is to use the natural binding affinity or recognition of biomolecules. Antibodies are often used in immunoaffinity chromatography, where the immobilized antibodies bind their corresponding epitope target to selectively remove it from a mixture.<sup>21</sup> One of the most well-known selective capture methods is avidin–biotin binding and has been exploited for a wide variety of biotechnologies.<sup>22,23</sup> However, this process requires the biotin to be attached to the protein of interest, thus requiring site-specific chemical reactivity. This method also suffers from multipoint modification since the target contains several copies of the same residue. Furthermore, the binding of these molecules is noncovalent and reversible under certain conditions. Specifically, the chemical and structural integrity of streptavidin would be susceptible to certain surface chemistries. Finally, these methods require that samples be engineered to contain the proper binding moieties, making them unamendable to most naturally occurring samples.

Aside from building specific reactive moieties into a peptide sequence through chemical synthesis, other strategies have been reported to create single-point modification and immobilization through the C-terminus. One approach employs the use of photoredox catalysis and exploits the difference in oxidation potentials between internal and C-terminal carboxylates to obtain selective C-terminal functionalization.<sup>24</sup> Enzyme-catalyzed protein labeling involving the use of a natural enzyme, often involved in post-translational modification, has also been put forth as an approach for tagging proteins of interest with a ligand or affinity reagent, such as biotin<sup>25</sup> or azides.<sup>26</sup> Azides are of particular interest because they can undergo a variety of efficient immobilization reactions such as the Staudinger ligation<sup>27,28</sup> or copper-catalyzed alkyne-azide cycloaddition (CuAAC).<sup>29,30</sup> Although enzyme-catalyzed protein labeling can be an effective tool for selective modification, it requires that the proteins of interest

contain specific residues or sequences to be recognized by the tagging enzyme. Herein, we detail a new general strategy for well-controlled peptide immobilization that is suitable for selective C-terminal conjugation of peptides that are generated by protease cleavage of a polypeptide immediately following a lysine residue in the amino acid sequence, thereby generating peptides that contain a single lysine residue located at the C-terminus. In this study, we used a synthesized peptide sequence with a lysine at its C-terminus to simulate such digested peptide fragments. A custom phenyl isothiocyanate containing an alkyne handle selectively reacts with the lysine and N-terminus primary amines and does not react with other amino groups, like the guanidinium group on arginine. Due to the nature of the protease digestion, the only primary amines on each fragment should be the C-terminal lysine and the N-terminus. As a result, each fragment should contain two alkynes after the reaction is complete. Exposing the double-modified fragments to acid causes selective cleavage of the N-terminus due to the formation of an energetically favorable five-membered ring, while the modified C-terminus lysine remains unchanged. The modified peptides were then immobilized on silane-functionalized silicon wafers through CuAAC reaction with the surface-bound azide groups. We further demonstrate that our strategy of building controlled, peptide interfaces through sequential self-assembled monolayer formation preserves the accessibility of the N-terminus of the surface-bound peptides for further chemical reactions by attaching a fluorine-containing molecule, which was detectable on the surface by X-ray photoelectron spectroscopy (XPS) analysis.

## 2. MATERIALS AND EXPERIMENTAL PROCEDURES<sup>†</sup>

**2.1. Chemicals and Instrumentation.** Tetrahydrofuran (THF), 4-ethynylaniline, diethyl ether (Et<sub>2</sub>O), tert-butanol (tBuOH), 4-toluenesulfonyl chloride (TsCl), pyridine, triethylamine (TEA), CuBr, *N,N,N',N'',N'''*-pentamethyldiethylenetriamine (PMDETA), 3,5-bis(trifluoromethyl)phenyl isothiocyanate (F<sub>6</sub>PITC), and trifluoroacetic acid (TFA) were ordered from Sigma-Aldrich and used as received. Ethyl acetate, hexanes, and carbon disulfide were ordered from VWR. Sodium azide (NaN<sub>3</sub>) was ordered from J.T. Baker Chemical Co. 11-Bromoundecyltrichlorosilane was ordered from Gelest, Inc. Reactions were carried out under an inert atmosphere of argon or nitrogen with dry solvents, using anhydrous conditions unless otherwise stated. Toluene was dried over molecular sieves (4 Å) for at least 24 h prior to use. Reagents were purchased at the highest commercial quality and used without further purification unless otherwise stated. Yields refer to chromatographically and spectroscopically (<sup>1</sup>H NMR) homogeneous material unless otherwise stated.

Flash column chromatography was performed using Silicycle Silica Gel 60 Å (40–53) μm. Analytical thin-layer chromatography (TLC) was performed using Merck Silica Gel 60 Å F-254 precoated plates (0.25 mm thickness). Preparatory HPLC (P-HPLC) was performed with a single-wavelength detector using an Xselect CSH OBD preparatory column (5 μm beads, 10 mm diameter × 250 mm length, 130 Å pore size). Variable-angle spectroscopic ellipsometry (VASE) data were obtained with an M-2000D series spectroscopic ellipsometer (J. A. Woollam, Inc., Lincoln, NE) with multiple angles of incidence (45°, 60°, and 75°) and fit to a Cauchy model to determine the thickness of the layers. Atomic force microscopy (AFM) images were collected using a Bruker Dimension Icon operating in ScanAsyst mode using a ScanAsyst-Air probe with a nominal tip radius of 2 nm and a cantilever spring constant of 0.4 N m<sup>-1</sup>. Root-mean-square (RMS) roughness was determined using the roughness function within the NanoScope analysis software after applying a third-order flattening function. All film thicknesses and

RMS roughness measurements (VASE and AFM) are reported as an average of at least three measurements with error as one standard deviation of the mean.  $^1\text{H}$  1D, total correlation spectroscopy (TOCSY),  $^1\text{H}$ ,  $^{13}\text{C}$  heteronuclear single quantum coherence (HSQC), and  $^1\text{H}$ ,  $^{15}\text{N}$  heteronuclear multiple quantum coherence (HMQC) nuclear magnetic resonance (NMR) spectra were collected on a Bruker 600 MHz AVANCE I NMR spectrometer with a room-temperature, triple-resonance TXI probe. Matrix-assisted laser desorption/ionization time-of-flight (MALDI-TOF) mass spectrometry was performed on a Bruker Daltonics Microflex apparatus in positive-ion mode using  $\alpha$ -cyano-4-hydroxycinnamic acid (CHCA) matrix. Ultraviolet-ozone (UVO) treatment of the samples was conducted using a UVO-Cleaner (Model 342, Jelight Company, Inc.). XPS measurements were performed using a Kratos Axis Ultra DLD spectrometer with a monochromated Al K $\alpha$  source. X-ray photoelectron spectroscopy (XPS) was performed on a Kratos AXIS Ultra DLD X-ray photoelectron spectrometer with a monochromated Al K $\alpha$  source operating at 1486.6 eV and 140 W. The base pressure of the sample analysis chamber was  $\approx 3.0 \times 10^{-9}$  Pa, and spectra were collected from a nominal spot size of  $300 \mu\text{m} \times 700 \mu\text{m}$ . Atomic composition was determined from survey scans over a binding energy range of (0–1200) eV, pass energy of 160 eV, step size of 0.5 eV, dwell time of 0.1 s, and with charge neutralizer off. Peak fitting was performed on high-resolution scans of the C 1s and N 1s regions collected using a pass energy of 40 eV, step size of 0.1 eV, and sweep time of 0.3 s. All XPS data analysis was performed using the CasaXPS software package.

**2.2. Peptide Synthesis (Synthesis of 1).** Short peptide strands were synthesized by solid-phase peptide synthesis by conventional methods. In short, the peptides used in this study were synthesized on a Gyros Protein Technologies Tribute Peptide Synthesizer. Gyros Protein Technologies and Novabiochem amino acids were used for the GFGVVRTK peptide sequence. HCTU (O-(1H-6-Chlorobenzotriazole-1-yl)-1,1,3,3-tetramethyluronium hexafluorophosphate) was used as the coupling reagent and added to each amino acid. A 0.31-substituted Fmoc-Lys(Boc)-Wang Resin was placed into a reaction vessel. The peptide was synthesized on a 10  $\mu\text{mol}$  scale starting with the N-terminus and was first linked to the lysine resin. After the synthesis was complete, the peptide was cleaved from the lysine resin for 3 h using 3 mL of TFA/phenol/water/triisopropylsilane (88/5/5/2 by volume fraction). Ice-cold diethyl ether was added to the peptide solution and placed in dry ice for 10 min. The peptide solution was centrifuged and decanted. This was repeated three times with the addition of ice-cold diethyl ether before each centrifuge round. After three centrifuge rounds, the peptide was dried under nitrogen overnight. A Waters HPLC fitted with an Xselect CSH OBD preparatory column was used to purify the peptide. Separation was performed with a linear solvent gradient from 5% to 100% B over a 90 min period at a flow rate of 2.5 mL/min. Solvent A was 0.1% trifluoroacetic acid (TFA) in water (by volume fraction), and solvent B was 0.1% TFA in acetonitrile (by volume fraction). The purified peptide was identified by MALDI-TOF and lyophilized.  $m/z$  calcd for  $[\text{M} + \text{H}]^+$ ,  $\text{C}_{34}\text{H}_{57}\text{N}_{11}\text{O}_9$ , 764.44 Da, found  $m/z$  764.69 Da (Figure S1a).  $^1\text{H}$  NMR (600 MHz, dimethyl sulfoxide (DMSO)- $d_6$  with 0.05% TMS (by volume fraction), 25  $^\circ\text{C}$ ) is shown in Figure S2a with labeled protons as follows:  $\delta$  0.84 (6H, dd,  $J = 16.2, 6.5$  Hz, H1), 1.06 (3H, d,  $J = 6.1$  Hz, H2), 1.31–1.39 (2H, m, H3), 1.50–1.56 (2H, m, H4), 1.50–1.65 (2H, m, H5), 1.65–1.73 (2H, m, H6), 1.75–1.83 (2H, m, H7), 1.95–2.00 (1H, m, H8), 2.73–2.78 (2H, m, H9), 2.76–2.83 (1H, m, H10), 3.05–3.12 (1H, m, H11), 3.06–3.12 (2H, m, H12), 3.77–3.86 (2H, m, H13), 4.01–4.04 (1H, m, H14), 4.06–4.12 (1H, m, H15), 4.20–4.27 (1H, m, H16), 4.38–4.42 (1H, m, H17), 4.57–4.65 (1H, m, H18), 4.76–4.98 (1H, br, H19), 7.76 (2H, br, H20), 7.90 (1H, s, H21), 7.93–8.26 (1H, br, H22), 8.24 (1H, s, H23), 8.55 (1H, s, H24), 8.76 (1H, s, H25).

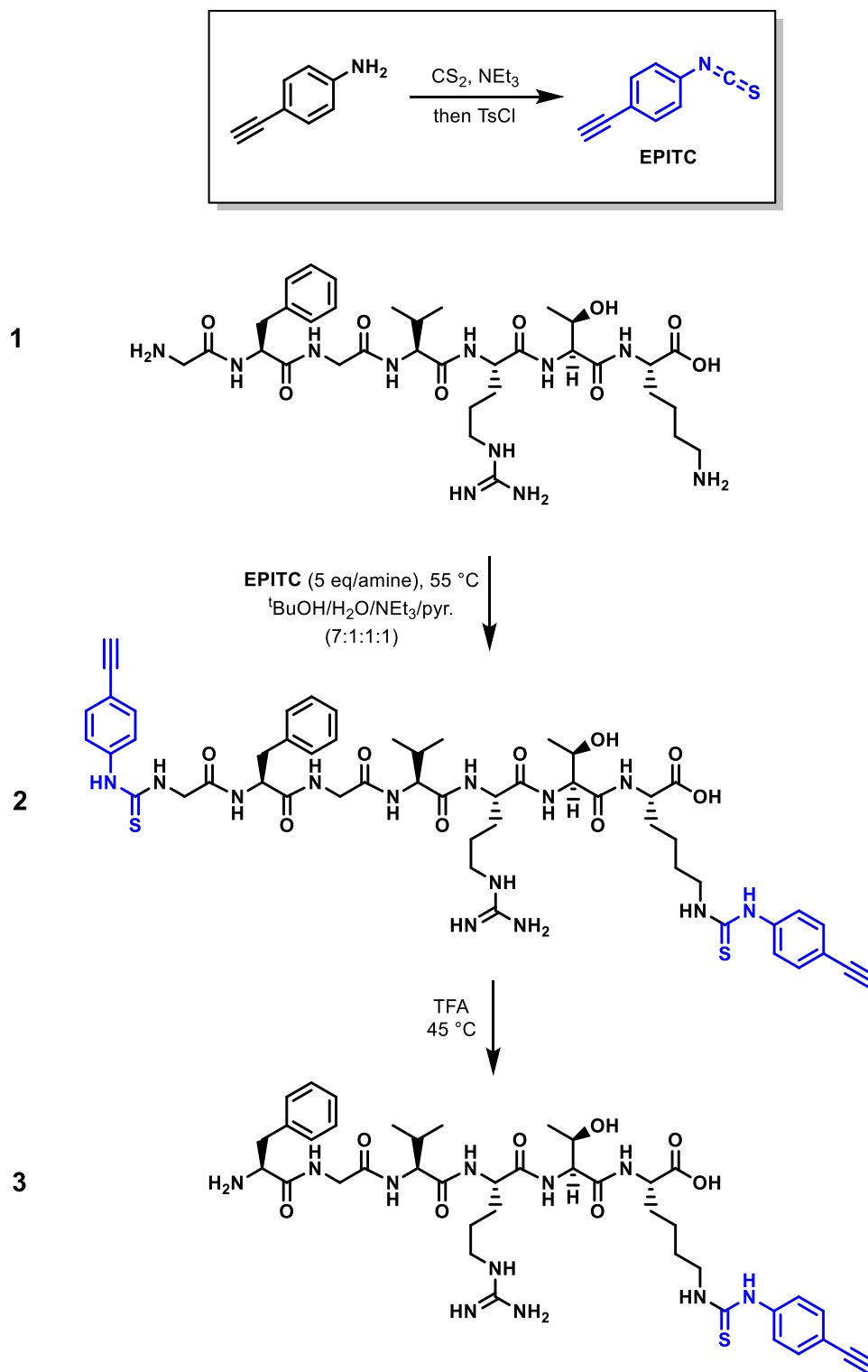
**2.3. Synthesis of 4-Ethynylphenyl isothiocyanate (EPITC).** EPITC was synthesized according to the literature procedure.<sup>31</sup> In short, a 25 mL round-bottom flask outfitted with a septum was charged with 500 mg (4.3 mmol) of 4-ethynylaniline dissolved in 3.0 mL of dry THF. Triethylamine (TEA, 3.0 mL, 21.5 mmol) was added

to give a clear colorless solution that was cooled to 0  $^\circ\text{C}$  and placed under an inert atmosphere. Carbon disulfide (0.51 mL, 8.6 mmol) was added slowly. After the addition, the reaction was allowed to warm to 23  $^\circ\text{C}$  with stirring. The reaction became a bright orange-red color. After 12 h, 0.850 g (4.7 mmol) of TsCl was added and the reaction stirring was continued for an additional hour at 23  $^\circ\text{C}$ . The reaction was then diluted with 10 mL of 1 mol/L hydrochloric acid and extracted with ethyl acetate ( $3 \times 10$  mL). It was then dried over  $\text{Na}_2\text{SO}_4$  and concentrated. The crude material was purified by column chromatography (100% hexanes) to give 463 mg of a pale-yellow solid (68% yield) that matched literature characterization.

**2.4. Modification of Peptides with EPITC (Synthesis of 2).** A one-dram vial was charged with 0.5 mg (0.7  $\mu\text{mol}$ ) of peptide GFGVVRTK dissolved in 50  $\mu\text{L}$  of water, 350  $\mu\text{L}$  of  $t$ -BuOH, 50  $\mu\text{L}$  of pyridine, and 50  $\mu\text{L}$  of TEA (1/7/1/1 by volume fraction). EPITC (2.0 mg (12.6 mmol, ca. 10 equiv/amine)) was added to the clear colorless solution turning it faint yellow. The reaction was stirred at 55  $^\circ\text{C}$  for 2 h before cooling to 23  $^\circ\text{C}$ . The solvent was removed by passing air over the solution until only a crude waxy solid remained. The residue was washed with hexanes ( $3 \times 1$  mL) to remove excess EPITC. The product was identified by MALDI-TOF.  $m/z$  calcd for  $[\text{M} + \text{H}]^+$ ,  $\text{C}_{52}\text{H}_{67}\text{N}_{13}\text{O}_9\text{S}_2$ , 1082.47, found 1082.42 (Figure S1b).  $^1\text{H}$  NMR (600 MHz, DMSO- $d_6$  with 0.05% TMS (by volume fraction)), 25  $^\circ\text{C}$  shown in Figure S2b with labeled protons as follows:  $\delta$  0.83 (6H, dd,  $J = 20.7, 6.7$  Hz, H1), 1.04 (3H, d,  $J = 6.2$  Hz, H2), 1.32–1.40 (2H, m, H3), 1.49–1.53 (2H, m, H4), 1.53–1.71 (2H, m, H5), 1.63–1.75 (2H, m, H6), 1.85–1.90 (2H, m, H7), 1.94–1.98 (1H, m, H8), 2.80 (1H, t,  $J = 11.5$  Hz, H9), 3.06–3.12 (2H, m, H10), 3.05–3.10 (1H, m, H11), 3.38–3.43 (2H, m, H12), 3.67–3.80 (2H, m, H13), 3.81–3.85 (1H, m, H14), 4.04–4.08 (2H, m, H15), 4.08–4.11 (1H, dd,  $H_z = 15.0, 6.6$  Hz, H16), 4.22–4.26 (1H, m, H17), 4.45 (1H, q,  $J = 6.3$  Hz, H18), 4.53–4.57 (1H, m, H19), 4.79–4.88 (1H, br, H20), 7.44–7.56 (1H, br, H21), 7.81 (1H, s, H22), 7.95 (1H, s, H23), 8.14 (1H, s, H24), 8.39 (1H, br, H25), 8.44 (1H, d,  $J = 8.4$  Hz, H26), 9.66 (1H, s, H27), 10.15 (1H, s, H28).

**2.5. Removal of N-terminus EPITC (Synthesis of 3).** The functionalized peptide residue from the above was dissolved in 0.5 mL of TFA in a one-dram vial and heated to 45  $^\circ\text{C}$  for 1 h and then cooled to 23  $^\circ\text{C}$ . The reaction was concentrated by blowing air over the surface until only a waxy solid remained. The crude material was washed with diethyl ether ( $3 \times 1$  mL). The product was identified by MALDI-TOF.  $m/z$  calcd for  $[\text{M} + \text{H} + \text{H}_2\text{O}]^+$ ,  $\text{C}_{41}\text{H}_{62}\text{N}_{11}\text{O}_9\text{S}$ , 884.44, found 884.22 (Figure S1c).  $^1\text{H}$  NMR (600 MHz, DMSO- $d_6$  with 0.05% TMS (by volume fraction), 25  $^\circ\text{C}$ ) shown in Figure S2c with labeled protons as follows:  $\delta$  0.85 (6H, dd,  $J = 19.8, 6.4$  Hz, H1), 1.06 (3H, d,  $J = 6.2$  Hz, H2), 1.32–1.39 (2H, m, H3), 1.44–4.55 (2H, m, H4), 1.52–1.56 (2H, m, H5), 1.53–1.72 (2H, m, H6), 1.63–1.75 (2H, m, H7), 1.94–1.98 (1H, m, H8), 2.93–2.98 (1H, m, H9), 3.07–3.11 (2H, m, H10), 3.09–3.13 (1H, m, H11), 3.84–3.89 (2H, m, H12), 3.95–3.98 (1H, m, H13), 4.09 (1H, br, H14), 4.11–4.15 (2H, m, H15), 4.19–4.23 (1H, m, H16), 4.25–4.29 (1H, m, H17), 4.33–4.39 (1H, m, H18), 4.85 (1H, br, s, H19), 7.54 (1H, s, H20), 7.77 (1H, s, H21), 7.94–8.02 (1H, m, H22), 7.99–8.08 (1H, m, H23), 8.13 (2H, br, H24), 8.21–8.27 (1H, m, H25), 8.39–8.42 (1H, m, H26), 8.69–8.72 (2H, m, H27), 9.07 (1H, s, H28).

**2.6. Generation of Azide-Functionalized Surface.** The generation of azide-functional surfaces was adapted from previous reports in the literature.<sup>32</sup> Prior to functionalization, (100)-oriented silicon wafers (University wafer, test grade, N-type, 0–100  $\Omega$  cm specific resistivity, 500  $\mu\text{m}$  thickness, 100 mm diameter) were cut into 1 cm  $\times$  1 cm pieces and were cleaned by sonication in acetone, ethanol, and water for 10 min each. After sonication, the surfaces were dried with nitrogen and UVO for 30 min. The surfaces were removed and used immediately. 11-Bromoundecyltrichlorosilane (35 mg, 0.1 mmol) was dissolved in 20 mL of anhydrous toluene. Freshly cleaned surfaces were completely submerged at 23  $^\circ\text{C}$  for 16 h. The surfaces were then removed from solution, rinsed and sonicated in toluene, and dried with an argon gas (Ar) steam. Subsequent azide functionalization was done by submerging the sample in oversaturated sodium azide (20 mg  $\text{NaN}_3$ ) in 2 mL of anhydrous dimethylforma-

Scheme 1. Synthesis of EPITC and Selective Modification of LysC Generated Peptides at the C-Terminus<sup>a</sup>

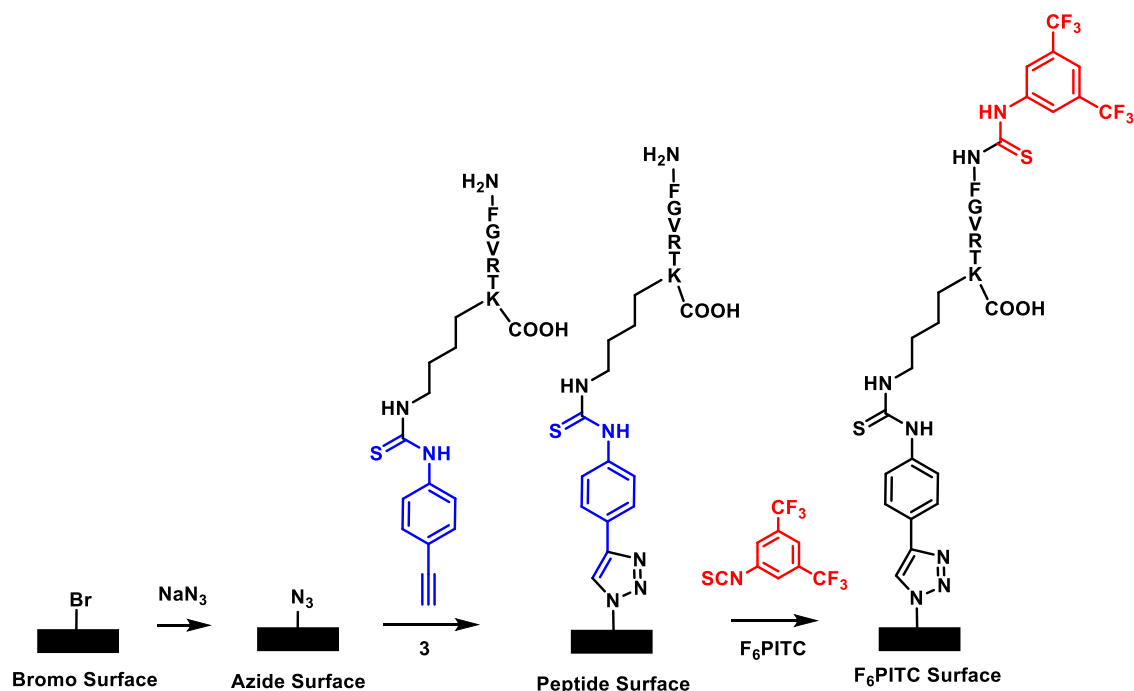
<sup>a</sup>1: unmodified peptide GFGVRTK, 2: difunctionalized peptide, 3: C-terminus-modified peptide.

mide (DMF) for 24 h. The surfaces were sonicated in DMF and rinsed with DMF, acetone, and 18.2 MΩ-cm resistance water. The surfaces were then analyzed with ellipsometry, AFM, and XPS.

**2.7. Peptide Immobilization.** Peptide (200 μg) was dissolved in 2.0 mL of DMF. The solution was sparged with argon for 25 min. CuBr (2.5 mg, 17.4 μmol) and PMDETA (20 μL, 95.8 μmol) were then added, and the solution was sparged for an additional 10 min, during which time the solution became green. An azide-functionalized

surface was then submerged in this solution while keeping the reaction vessel under an inert atmosphere. The vessel was placed in a prewarmed oil bath at 55 °C and heated for 16 h. After the reaction, the substrate was rinsed and sonicated with DMF for 10 min and then rinsed with a copious amount of acetone and DI water. Samples could be stored under ambient conditions submerged in a solution of water for several days.

**Scheme 2. Surface Immobilization of Alkyne-Functionalized Peptide (3 from Scheme 1) onto Azide-Terminated Silane Surface, Followed by Subsequent Addition of F<sub>6</sub>PITC to Demonstrate the Activity of the Peptide N-Terminal Primary Amine**



**2.8. F<sub>6</sub>PITC Tagging on the Peptide Surface.** F<sub>6</sub>PITC functionalization on peptide-immobilized surfaces was performed using a modified literature procedure.<sup>33</sup> In brief, 25 mg (92.2 μmol) of 3,5-bis(trifluoromethyl)phenyl isothiocyanate (F<sub>6</sub>PITC) and 15 mg of TEA (0.148 mmol) were dissolved in 2 mL of DMSO, yielding a yellow solution. The peptide-functionalized surface was submerged in the solution at room temperature for 16 h. The surface was removed, washed with DMSO, and sonicated in DMSO, and again washed with acetone before drying with an Ar stream. The surface was analyzed with XPS.

### 3. RESULTS AND DISCUSSION

#### 3.1. Alkyne Modification at the C-Terminus of Protease-Digested Peptides with C-Terminal Lysines.

To achieve single-point attachment of protease-digested peptides via the C-terminus, we selectively modified the C-terminus lysine of the peptide with a click chemistry functional group by exploiting known Edman chemistry (Scheme 1). The thiourea linkage added to the peptide at the C-terminus in this way has been shown to be effective at immobilizing peptides and is sufficiently stable to iterative rounds of surface chemistry.<sup>34</sup>

To demonstrate this approach, we synthesized a variant of the Edman degradation reagent phenyl isothiocyanate EPITC from 4-ethynylaniline to contain a clickable alkyne group. We then synthesized a 7-AA-long peptide sequence FGVR<sup>1</sup>K (m/z 764.04 [M + H]<sup>+</sup>, Figure S1a) by solid-phase synthesis methods. This peptide was used to represent a typical peptide fragment after protease digestion, which contains a variety of AAs and a lysine that is present at the C-terminus. Scheme 1 shows the modification of the C-terminus lysine by reaction with EPITC. Exposing peptide 1 to excess EPITC under basic conditions resulted in quantitative conversion to a difunctionalized material 2 where both the N-terminus and C-terminus lysine transformed into thioureas, as confirmed by MALDI-TOF (m/z 1082.54 [M + H], Figure S1b). We gently heated the material in neat TFA to cleave off the *n*-terminal glycine

AA containing the extra alkyne group and convert 2 to 3.<sup>35</sup> Under these conditions, the other thiourea formed with lysine cannot cyclize and therefore remains unaffected. The isolated product 3 showed an m/z of 884.06 [M + H + H<sub>2</sub>O]<sup>+</sup> (Figure S1c) that matches the theoretical value.

<sup>1</sup>H NMR (Figure S2) was used to confirm the structure of the modified peptide. After the EPITC functionalization of 1, three new thiourea protons, H<sub>25</sub>, H<sub>27</sub>, and H<sub>28</sub> appeared in 2, which indicates the formation of thiourea bonds in 2 at both ends of the peptide. After the TFA cleavage reaction, the N-terminus α proton H<sub>15</sub> and the N-terminus thiourea protons H<sub>25</sub> and H<sub>28</sub> in 2 disappeared and the phenylalanine amide proton was changed from a doublet at 8.44 ppm (H<sub>26</sub> in 2) to a singlet at 8.13 ppm (H<sub>24</sub> in 3). This observation verified the removal of the N-terminus PITC and glycine and the formation of a new N-terminal amine. Meanwhile, the thiourea protons H<sub>26</sub> and H<sub>28</sub> along with other lysine protons H<sub>3</sub>, H<sub>5</sub>, H<sub>6</sub>, H<sub>15</sub>, H<sub>16</sub>, and H<sub>22</sub> remain clearly visible in 3, confirming the intactness of the modified C-terminus lysine. In addition, no residual NMR signal of 1 was observed in 3, which suggests an overall quantitative conversion. The combined NMR data confirm that by exploiting the TFA cleavage reactivity difference between the α-amine and the ε-amine, the EPITC modification can be successfully localized to the C-terminus.

The addition of EPITC was initially carried out in methanol; however, the residual solvent proved difficult to remove and was detrimental in the subsequent acid-catalyzed cleavage reaction. Under the harshly acidic environment, methanol esterified the C-terminus, and any other acidic residues, to give a methyl ester as seen by MALDI-TOF (Figure S4). Performing the reaction using deuterated methanol gave a product whose mass was three atomic mass units heavier, confirming that methanol was responsible for the esterified product. This problem was resolved by switching to *tert*-butanol since the steric bulk prevents the base from acting as a nucleophile at the C-terminus. Furthermore, *tert*-butyl esters

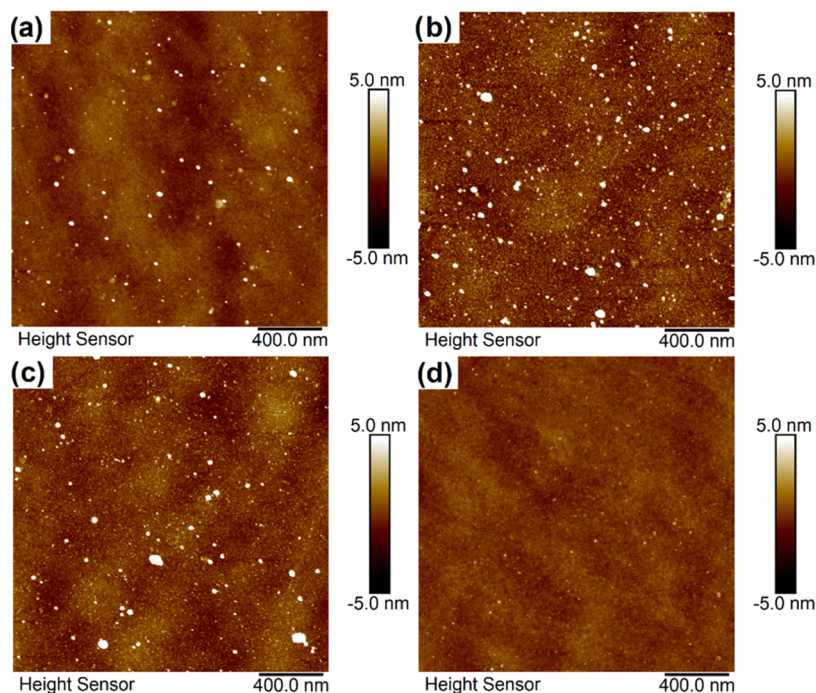


**Figure 1.** AFM height results of (a) azide-functionalized silane surface, (b) peptide-immobilized surface, (c) fluorine-tagged peptide surface, and (d) azide surface after peptide physisorption (control).

are known to hydrolyze to acids when exposed to TFA. Upon switching to the bulkier solvent, the target product mass was observed by MALDI-TOF.

**3.2. C-Terminus Selective Immobilization of Peptide on Surface via Click Chemistry.** Copper-catalyzed click chemistry was used to immobilize the alkyne-functionalized peptide onto the azide-containing surface through a covalent bond (Scheme 2). A bromo-terminated silane surface was first made on a silicon wafer. The azide-terminated surface was generated by reacting the bromo surface with a saturated solution of  $N_3$  in DMF. The surface was then reacted with **3** via the CuAAC reaction to form the peptide-immobilized surface. After C-terminus modification, the peptide showed reduced solubility in water, but was readily soluble in DMF. PMDETA was found to be a reliable ligand for the formation of a catalytic copper complex. We further tested the integrity of the immobilized peptides on the surface and availability of the N-terminus for further binding and/or chemistry by chemically adding the fluorine-containing compound  $F_6$ PITC. The surface transformations were quantified at each step chemically via XPS, and the layer thickness and roughness were characterized by ellipsometry and AFM roughness measurements.

The ellipsometric thicknesses of the Br- and azide-terminated surfaces were found to be  $(2.5 \pm 0.2)$  nm and  $(2.3 \pm 0.2)$  nm, respectively, which correspond to monolayer thicknesses of the silane-anchored layers (calculated to be 2.2 nm using the fully extended 3D molecular structure). In addition, the AFM height scan of the azide surface (Figure 1a) shows a homogeneous surface, containing some small aggregates (radius < 30 nm), with an RMS roughness of  $(0.49 \pm 0.01)$  nm measured at the featureless regions excluding large aggregates. The surface thickness after peptide immobilization was measured to be  $(3.9 \pm 0.2)$  nm (ellipsometry data), with a 1.6 nm increase from the azide surface. This increase matches the calculated length of 1.8 nm of a single layer of peptide chain (extended 3D molecular structure).

AFM roughness of the featureless area also increased to  $(0.95 \pm 0.11)$  nm (Figure 1b and summarized in Table 1).

**Table 1. Surface Thickness Measured by Ellipsometry and Surface Roughness from the Featureless Regions Measured by AFM Topology of the Surface Substrate at Different Functionalization Stages<sup>a</sup>**

surface terminal group	thickness (nm)	RMS roughness (nm)
bromo	$2.5 \pm 0.2$	$0.53 \pm 0.08$
azide	$2.3 \pm 0.2$	$0.49 \pm 0.01$
peptide	$3.9 \pm 0.2$	$0.95 \pm 0.11$
$F_6$ PITC	$3.1 \pm 0.2$	$0.73 \pm 0.05$
azide control <sup>b</sup>	$1.8 \pm 0.1$	$0.38 \pm 0.03$

<sup>a</sup>Error in the table is representative of one standard deviation of all measurements taken. <sup>b</sup>Azide surface after incubating in alkyne-modified peptide DMF solution and reacting with  $F_6$ PITC.

Representative spectroscopic data acquired by XPS elemental analysis after each reaction step are shown in Figure 2. First, the XPS spectrum of the bromo silane-functionalized surface shows a Br 3d signal at 68 eV and a strong C 1s signal at 285 eV, indicating the formation of a self-assembled monolayer on the silicon surface. The Br signal is replaced with an N 1s peak at 403 eV, after reaction with  $NaN_3$ , suggesting a complete conversion of the surface to azide, which was then functionalized with the modified peptide. Table 2 shows the theoretical and measured elemental ratio of C to N of the azide- and peptide-functionalized surfaces, calculated from their chemical formulas. As can be seen, the measured C/N ratio of  $15.8 \pm 4.3$  of the azide surface is significantly higher than the theoretical value (3.7). This could be a result of X-ray-induced azide degradation during the XPS measurements.<sup>36</sup> This hypothesis is supported by the lower measured C/N ratio of  $12.3 \pm 0.4$  for the peptide surface after the azides were reacted to form the more stable triazole. Residual Cu, used in

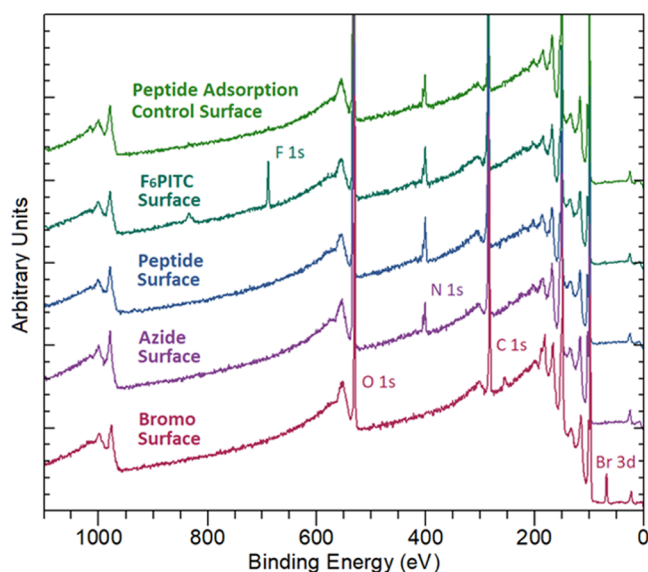


**Figure 2.** XPS elemental analysis survey results of the sample surface at different reaction stages, from bottom to top: bromo-terminated silane surface (red trace), azide-functionalized silane surface (purple trace), C-terminus-selective peptide-immobilized surface (blue trace),  $F_6$ PITC-tagged peptide surface (dark green trace), and peptide physisorption control on azide surface after reacting with  $F_6$ PITC (light green trace). All spectra are normalized to the peak of the C 1s region at 284.5 eV.

excess in click reaction, could interfere with the fluorescence measurements of the peptide surface immobilization-based peptide analysis but was avoided by adding excess PMDETA in the click reaction and no Cu signal was displayed in the XPS (Figure 2, Cu 2p signal usually found at  $\approx$  932 eV).

To further interrogate the surface elemental composition and chemistry, high-resolution N 1s and C 1s XPS spectra were obtained. The N 1s region of the azide surface shows two peaks at 400.3 and 404.0 eV (Figure 3a) that correspond to the terminal nitrogen (indicated by the  $N^-$  in the shown resonance structure) and the central, electron-deficient  $N^+$  from the azido group, respectively.<sup>37</sup> Their area ratio of 2:1 agrees with calculations for this system. After peptide immobilization, the N 1s region shows new signals, which were deconvoluted into three peaks at (399.8, 401.8, and 398.3) eV assigned to the peptide amides  $N-C=O$ , the protonated amine  $NH_3^+$  of peptides, and the aromatic  $C=N$  of the triazole, respectively. In addition, compared to the azide surface, the C 1s region of the peptide surface shows an emerging peak at 288.0 eV that corresponds to the amide  $N-C=O$  group and an increase of the existing C-N, C-O component at 285.7 eV (see Table 3). Taken together, these data support the conclusion that the peptide is covalently immobilized via the azide groups.

### 3.3. Testing N-Terminal Activity of Surface-Immobilized Peptides.

To demonstrate the integrity and activity of

the N-terminus amine of the immobilized peptides, we added a molecule with six fluorine atoms, 3,5-bis(trifluoromethyl)-phenyl isothiocyanate ( $F_6$ PITC), to tag via N-terminus amine the peptide with a fluorine element. Fluorine has a fairly high relative sensitivity factor (RSF) and is easily detected in XPS measurements. After reaction with  $F_6$ PITC (TEA in DMSO), the XPS survey scan shows a pronounced F 1s along with its KLL (Auger) peaks at 687.6 eV and 833.2 eV, respectively (Figure 3f), indicating covalent functionalization of the N-terminus amine. The calculated C/F ratio  $11.4 \pm 1.7$  is in good agreement with a theoretical value of 10.2 for a nearly fully functionalized surface. Our data indicate that about 90% of the surface bond peptides have an active N-terminus, based on XPS elemental analysis.

These conclusions were further supported by high-resolution XPS data. N 1s scan of the  $F_6$ PITC functionalized peptide surface in Figure 3c showed no visible change in  $NH_2$ ,  $N-C=O$ , or  $C=N$  peak in the fitted components after reacting with the peptide surface as expected. On the other hand, the C 1s regional scan of the  $F_6$ PITC surface showed an occurrence of a C-F component 292.6 eV (Figure 3f). The area percentages of the C 1s components C-C, C=C:C-N, C-O:N-C=O:C-F are measured to be (5.7:3.0:1.0:3.3)%, respectively, which closely matches the calculated ratio of a fully and uniformly converted surface (assuming 100% conversion in each step) of (5.9:2.5:1.3:3.3)%.

The surface thickness of the  $F_6$ PITC surface was measured to be  $(3.1 \pm 0.2)$  nm by ellipsometry, which is slightly lower than the peptide surface thickness (Table 1). Surface roughness measured by AFM also showed a slightly decreased value of  $(0.73 \pm 0.05)$  nm (Figure 1c). This could be a result of a change in the orientation of the monolayer from a largely upright orientation, i.e., more aligned along the surface normal when terminated by the more polar peptide, to a less upright, more canted orientation, i.e., away from the surface normal, induced by the addition of the now terminal hydrophobic  $F_6$ PITC component.

**3.4. Peptide Physisorption Control.** To determine the extent of nonspecific peptide adsorption or physisorption onto our surfaces, we carried out a control experiment by reacting the alkyne-terminated peptide with the azide surface in the absence of CuBr catalyst. Ellipsometry measurements of the resulting surface showed no thickness increase after 24 h of interaction with the modified peptide solution in DMF at  $(1.8 \pm 0.1)$  nm, as shown in Table 1. AFM topologic results also showed no increase in surface roughness (Table 2) and even show a reduced number of aggregated features (Figure 1d), which is in contrast to that of the peptide surface. The surface that was exposed to peptide without CuBr was then treated with  $F_6$ PITC in the same manner as above and analyzed with XPS. The XPS spectrum (Figure 2 top spectrum) showed no observable F 1s signal. These controls demonstrate that the reported peptide immobilization method is free from

**Table 2. Theoretical Chemical Formula, Measured Atomic Percentages of C, N, F, and Calculated and Measured Elemental Ratios of C/N and C/F of the Substrate Surface at Different Stages<sup>a</sup>**

surface terminal group	chemical formula	C (%)	N (%)	F (%)	C/N calculated	C/N measured	C/F calculated	C/F measured
azide	$C_{11}H_{22}Cl_3N_3Si$	94.0	6.0	0	3.7	$15.8 \pm 4.3$		
peptide	$C_{52}H_{81}Cl_3N_{14}O_8SSi$	92.5	7.5	0	3.7	$12.3 \pm 0.4$		
$F_6$ PITC	$C_{61}H_{83}Cl_3F_6N_{15}O_8S_2Si$	84.8	7.7	7.4	4.1	$11.0 \pm 0.6$	10.2	$11.4 \pm 1.7$

<sup>a</sup>Reported error is one standard deviation of the mean.

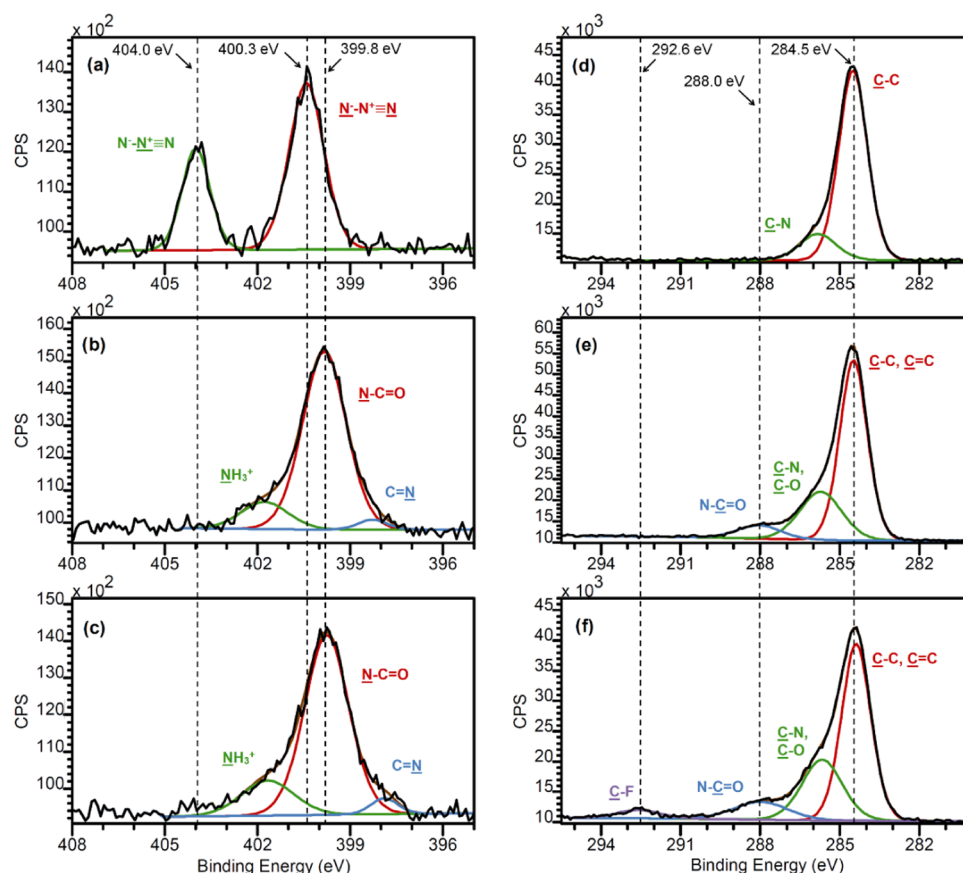


**Figure 3.** Representative high-resolution XPS N 1s region of (a) azide-functionalized surface, (b) peptide-immobilized surface, (c) peptide surface after reacting with F<sub>6</sub>PITC; and high-resolution XPS C 1s region of (d) azide surface, (e) peptide surface, and (f) F<sub>6</sub>PITC surface.

**Table 3. XPS C 1s Regional Scan Component Area Percentage Ratio from Substrate Surface at Different Functionalization Stages**

surface terminal group	C–C %	C–N, C–O % <sup>a</sup>	N–C=O %	C–F %
azide	79.7 ± 4.6	20.3 ± 4.6		
peptide	62.4 ± 2.5	30.2 ± 2.7	7.4 ± 0.7	
F <sub>6</sub> PITC	56.7 ± 3.0	30.0 ± 2.8	9.9 ± 0.7	3.3 ± 0.8

<sup>a</sup>Refers to C–N % for the surface with azide terminal group and C–N & C–O % for surfaces with peptide and F<sub>6</sub>PITC terminal groups.

interference from peptide physisorption and can potentially be used in quantitative analysis to determine N-terminus fidelity in future studies.

#### 4. CONCLUSIONS

In summary, we propose a new method for selectively modifying the C-terminus of peptides that are generated from protease digestion of natural biological sources. We have successfully attached an alkyne group to the peptide C-terminus via isothiocyanate chemistry, which was then used to create a single-point attachment to the azide-functionalized surface. A facile and robust CuAAC reaction was used to create covalent immobilization. Peptide modification chemistry showed a quantitative conversion in each step, characterized by NMR and MALDI-TOF, and surfaces were thoroughly characterized by XPS, AFM, and ellipsometry. Finally, the immobilized peptides were shown to contain an active N-terminus capable of reacting with an isothiocyanate group and

the surfaces were free from physisorbed contaminations. While some limitations may be faced with certain post-translational modifications (PTMs), the chemistries which we describe are well characterized and generalizable to any peptide generated from protease-digested protein samples, where cleavage occurs on the carboxyl side of lysine residues, without the need for any further chemical modifications or protective groups. The chemistry allows for the single-point covalent attachment of peptides to surfaces while leaving the N-terminus free and is therefore well suited for use in emerging protein sequencing and peptide microarray technologies and could be extended to other surface morphologies such as microspheres and microfluidic channels. The method does sacrifice one N-terminal AA of each peptide. However, since most highly parallel sequencing techniques utilize oversampling of short peptide fragments, this loss of information should be minimal in most applications, particularly those sequencing techniques that are based on “shot-gun” approaches where genomic data are used to reconstruct the protein sequence.

#### ■ ASSOCIATED CONTENT

##### Supporting Information

The Supporting Information is available free of charge at <https://pubs.acs.org/doi/10.1021/acs.langmuir.2c00359>.

MALDI-TOF spectra from top to bottom: purified peptide 1, peptide after EPITC addition reaction 2, and after TFA cleavage reaction 3 (Figure S1); <sup>1</sup>H NMR of the purified peptide 1, double PITC-modified peptide 2, and single PITC modification product 3 (Figure S2);

NMR TOCSY spectra from top to bottom: purified peptide **1**, peptide after PITC addition reaction **2**, and after TFA cleavage reaction **3** (Figure S3); and MALDI spectra of double-modified peptide, removal of N-terminal PITC and C-terminal modification with MeOH, removal of N-terminal PITC and C-terminal modification with CD<sub>3</sub>OD, and reaction performed in <sup>t</sup>BuOH resulting in no C-terminal modification (Figure S4) (PDF)

## AUTHOR INFORMATION

### Corresponding Author

Sara V. Orski – National Institute of Standards & Technology, Gaithersburg, Maryland 20899, United States; [orcid.org/0000-0002-3455-0866](https://orcid.org/0000-0002-3455-0866); Email: [sara.orski@nist.gov](mailto:sara.orski@nist.gov)

### Authors

Tian Xie – National Institute of Standards & Technology, Gaithersburg, Maryland 20899, United States; Georgetown University, Washington, District of Columbia 20057, United States; University of Maryland - Institute for Bioscience and Biotechnology Research, Rockville, Maryland 20850, United States; Present Address: J-Star Research Inc, 6 Cedarbrook Dr, East Windsor, New Jersey 08512, United States

Alexandria Brady – University of Maryland - Institute for Bioscience and Biotechnology Research, Rockville, Maryland 20850, United States

Cecilia Velarde – University of Maryland - Institute for Bioscience and Biotechnology Research, Rockville, Maryland 20850, United States

David N. Vaccarello – National Institute of Standards & Technology, Gaithersburg, Maryland 20899, United States; University of Maryland - Institute for Bioscience and Biotechnology Research, Rockville, Maryland 20850, United States

Nicholas W. Callahan – University of Maryland - Institute for Bioscience and Biotechnology Research, Rockville, Maryland 20850, United States

John P. Marino – National Institute of Standards & Technology, Gaithersburg, Maryland 20899, United States; University of Maryland - Institute for Bioscience and Biotechnology Research, Rockville, Maryland 20850, United States

Complete contact information is available at:

<https://pubs.acs.org/10.1021/acs.langmuir.2c00359>

### Notes

The authors declare no competing financial interest. Official contribution of the National Institute of Standards & Technology; not subject to copyright in the United States.

## ACKNOWLEDGMENTS

This work was supported by NIST through its Innovations in Measurement Science program. T.X. was supported through a NIST Professional Research Experience Program (PREP) Postdoctoral Fellowship administered by Georgetown University. The authors thank Zvi Kelman, David Vanderah (IBBR), Kathryn Beers (NIST), and Christopher Stafford (NIST) for kindly sharing their knowledge in biochemistry, organic chemistry, and surface chemistry. They also thank

Robert Brinson and Nese Sari (IBBR) for providing their expertise in NMR instrumentation, and Kristen Steffens and Justin Gorham (NIST) for their expertise in XPS instrumentation.

## ADDITIONAL NOTE

<sup>1</sup>Certain commercial equipment, instruments, or materials are identified in this paper to specify the experimental procedure adequately. Such identification is not intended to imply recommendation or endorsement by the National Institute of Standards & Technology, nor is it intended to imply that the materials or equipment identified are necessarily the best available for the purpose.

## REFERENCES

- (1) Beyer, M.; Felgenhauer, T.; Ralf Bischoff, F.; Breitling, F.; Stadler, V. A Novel Glass Slide-Based Peptide Array Support with High Functionality Resisting Non-Specific Protein Adsorption. *Biomaterials* **2006**, *27*, 3505–3514.
- (2) Zhao, Y.; Pirrung, M. C.; Liao, J. A Fluorescent Amino Acid Probe to Monitor Efficiency of Peptide Conjugation to Glass Surfaces for High Density Microarrays. *Mol. BioSyst.* **2012**, *8*, 879–887.
- (3) Bhakta, S. A.; Evans, E.; Benavidez, T. E.; Garcia, C. D. Protein Adsorption onto Nanomaterials for the Development of Biosensors and Analytical Devices: A Review. *Anal. Chim. Acta.* **2015**, *872*, 7–25.
- (4) Shrestha, N.; Araújo, F.; Shahbazi, M. A.; Mäkilä, E.; Gomes, M. J.; Herranz-Blanco, B.; Lindgren, R.; Granroth, S.; Kukk, E.; Salonen, J.; Hirvonen, J.; Sarmiento, B.; Santos, H. A. Thiolation and Cell-Penetrating Peptide Surface Functionalization of Porous Silicon Nanoparticles for Oral Delivery of Insulin. *Adv. Funct. Mater.* **2016**, *26*, 3405–3416.
- (5) Kasálková, N. S.; Slepíčka, P.; Kolská, Z.; Hodačová, P.; Kučková, Š.; Švorčík, V. Grafting of Bovine Serum Albumin Proteins on Plasma-Modified Polymers for Potential Application in Tissue Engineering. *Nanoscale Res. Lett.* **2014**, *9*, No. 161.
- (6) Maskos, U.; Southern, E. Oligonucleotide Hybridizations on Glass Supports: A Novel Linker for Oligonucleotide Synthesis and Hybridisation Properties of Oligonucleotides Synthesised in Situ. *Nucleic Acids Res.* **1992**, *20*, 1679–1684.
- (7) Fodor, S. P. A.; Read, J. L.; Pirrung, M. C.; Stryer, L.; Lu, A. T.; Solas, D. Light-Directed, Spatially Addressable Parallel Chemical Synthesis. *Science* **1991**, *251*, 767–773.
- (8) Kumar, R. M. The Widely Used Diagnostics “DNA Microarray” - A Review. *Am. J. Infect. Dis.* **2009**, *5*, 214–225.
- (9) Reimer, U.; Reineke, U.; Schneider-Mergener, J. Peptide Arrays: From Macro to Micro. *Curr. Opin. Biotechnol.* **2002**, *13*, 315–320.
- (10) Szymczak, L. C.; Kuo, H. Y.; Mrksich, M. Peptide Arrays: Development and Application. *Anal. Chem.* **2018**, *90*, 266–282.
- (11) Callahan, N.; Tullman, J.; Kelman, Z.; Marino, J. Strategies for Development of a Next-Generation Protein Sequencing Platform. *Trends Biochem. Sci.* **2020**, *45*, 76–89.
- (12) Swaminathan, J.; Boulgakov, A. A.; Hernandez, E. T.; Bardo, A. M.; Bachman, J. L.; Marotta, J.; Johnson, A. M.; Anslyn, V. E.; Marcotte, E. M. Highly Parallel Single-Molecule Identification of Proteins in Zeptomole-Scale Mixtures. *Nat. Biotechnol.* **2018**, *36*, 1076–1091.
- (13) Rodrigues, S. G.; Marblestone, A. H.; Boyden, E. S. A Theoretical Analysis of Single Molecule Protein Sequencing via Weak Binding Spectra. *PLoS One* **2019**, *14*, No. e0212868.
- (14) Chen, D.; Disotuar, M. M.; Xiong, X.; Wang, Y.; Chou, D. H. C. Selective N-Terminal Functionalization of Native Peptides and Proteins. *Chem. Sci.* **2017**, *8*, 2717–2722.
- (15) Lim, C. Y.; Owens, N. A.; Wampler, R. D.; Ying, Y.; Granger, J. H.; Porter, M. D.; Takahashi, M.; Shimazu, K. Succinimidyl Ester Surface Chemistry: Implications of the Competition between Aminolysis and Hydrolysis on Covalent Protein Immobilization. *Langmuir* **2014**, *30*, 12868–12878.

- (16) MacBeath, G.; Schreiber, S. L. Printing Proteins as Microarrays for High-Throughput Function Determination. *Science* **2000**, *289*, 1760–1763.
- (17) Zhu, H.; Bilgin, M.; Bangham, R.; Hall, D.; Casamayor, A.; Bertone, P.; Lan, N.; Jansen, R.; Bidlingmaier, S.; Houfek, T.; Mitchell, T.; Miller, P.; Dean, R. A.; Gerstein, M.; Snyder, M. Global Analysis of Protein Activities Using Proteome Chips. *Science* **2001**, *293*, 2101–2105.
- (18) Cheung, C. L.; Camarero, J. A.; Woods, B. W.; Lin, T.; Johnson, J. E.; de Yoreo, J. J. Fabrication of Assembled Virus Nanostructures on Templates of Chemoselective Linkers Formed by Scanning Probe Nanolithography. *J. Am. Chem. Soc.* **2003**, *125*, 6848–6849.
- (19) Ferrero, V. E. v.; Andolfi, L.; di Nardo, G.; Sadeghi, S. J.; Fantuzzi, A.; Cannistraro, S.; Gilardi, G. Protein and Electrode Engineering for the Covalent Immobilization of P450 BMP on Gold. *Anal. Chem.* **2008**, *80*, 8438–8446.
- (20) Howard, C. J.; Floyd, B. M.; Bardo, A. M.; Swaminathan, J.; Marcotte, E. M.; Anslyn, V. E. Solid-Phase Peptide Capture and Release for Bulk and Single-Molecule Proteomics. *ACS Chem. Biol.* **2020**, *15*, 1401–1407.
- (21) Hedhammar, M.; Gräslund, T.; Hober, S. Protein Engineering Strategies for Selective Protein Purification. *Chem. Eng. Technol.* **2005**, *28*, 1315–1325.
- (22) Bayer, E. A.; Wilchek, M. The Use of the Avidin-Biotin Complex as a Tool in Molecular Biology. *Methods Biochem. Anal.* **1980**, *26*, 1–45.
- (23) Laitinen, O. H.; Nordlund, H. R.; Hytönen, V. P.; Kulomaa, M. S. Brave New (Strept)Avidins in Biotechnology. *Trends Biotechnol.* **2007**, *25*, 269–277.
- (24) Bloom, S.; Liu, C.; Kölmel, D. K.; Qiao, J. X.; Zhang, Y.; Poss, M. A.; Ewing, W. R.; Macmillan, D. W. C. Decarboxylative Alkylation for Site-Selective Bioconjugation of Native Proteins via Oxidation Potentials. *Nat. Chem.* **2018**, *10*, 205–211.
- (25) Cull, M. G.; Schatz, P. J. Biotinylation of Proteins in Vivo and in Vitro Using Small Peptide Tags. *Methods Enzymol.* **2000**, *326*, 430–440.
- (26) Gauchet, C.; Labadie, G. R.; Poulter, C. D. Regio- and Chemoselective Covalent Immobilization of Proteins through Unnatural Amino Acids. *J. Am. Chem. Soc.* **2006**, *128*, 9274–9275.
- (27) Köhn, M.; Breinbauer, R. The Staudinger Ligation - A Gift to Chemical Biology. *Angew. Chem., Int. Ed.* **2004**, *43*, 3106–3116.
- (28) Saxon, E.; Bertozzi, C. R. Cell Surface Engineering by a Modified Staudinger Reaction. *Science* **2000**, *287*, 2007–2010.
- (29) Lutz, J. F.; Zarafshani, Z. Efficient Construction of Therapeutics, Bioconjugates, Biomaterials and Bioactive Surfaces Using Azide-Alkyne “Click” Chemistry. *Adv. Drug Delivery Rev.* **2008**, *60*, 958–970.
- (30) Kolb, H. C.; Finn, M. G.; Sharpless, K. B. Click Chemistry: Diverse Chemical Function from a Few Good Reactions. *Angew. Chem., Int. Ed.* **2001**, *40*, 2004–2021.
- (31) Wong, R.; Dolman, S. J. Isothiocyanates from Tosyl Chloride Mediated Decomposition of in Situ Generated Dithiocarbamic Acid Salts. *J. Org. Chem.* **2007**, *72*, 3969–3971.
- (32) Chisholm, R.; Parkin, J. D.; Smith, A. D.; Hähner, G. Isothiourea-Mediated Organocatalytic Michael Addition-Lactonization on a Surface: Modification of SAMs on Silicon Oxide Substrates. *Langmuir* **2016**, *32*, 3130–3138.
- (33) Graf, N.; Lippitz, A.; Gross, T.; Pippig, F.; Holländer, A.; Unger, W. E. S. Determination of Accessible Amino Groups on Surfaces by Chemical Derivatization with 3,5-Bis(Trifluoromethyl)-Phenyl Isothiocyanate and XPS/NEXAFS Analysis. *Anal. Bioanal. Chem.* **2010**, *396*, 725–738.
- (34) Xu, G.; Shin, S. B. Y.; Jaffrey, S. R. Global Profiling of Protease Cleavage Sites by Chemoselective Labeling of Protein N-Termini. *Proc. Natl. Acad. Sci. U.S.A.* **2009**, *106*, 19310–19315.
- (35) Bailey, J. M. Chemical Methods of Protein Sequence Analysis. *J. Chromatogr. A* **1995**, *705*, 47–65.
- (36) Saad, A.; Abderrabba, M.; Chehimi, M. M. X-Ray Induced Degradation of Surface Bound Azido Groups during XPS Analysis. *Surf. Interface Anal.* **2017**, *49*, 340–344.
- (37) Poreba, R.; de los Santos Pereira, A.; Pola, R.; Jiang, S.; Pop-Georgievski, O.; Sedláková, Z.; Schönherr, H. “Clickable” and Antifouling Block Copolymer Brushes as a Versatile Platform for Peptide-Specific Cell Attachment. *Macromol. Biosci.* **2020**, *20*, No. e1900354.

## Recommended by ACS

### Synthetic Peptides in Doping Control: A Powerful Tool for an Analytical Challenge

Néstor Alejandro Gómez-Guerrero, Javier Eduardo García-Castañeda, *et al.*

OCTOBER 21, 2022  
ACS OMEGA

READ 

### Rapid Covalent Labeling of Membrane Proteins on Living Cells Using a Nanobody–Epitope Tag Pair

Chino C. Cabaltea, Ross W. Cheloha, *et al.*

SEPTEMBER 15, 2022  
BIOCONJUGATE CHEMISTRY

READ 

### Protein-Labeling Fluorescent Probe Reveals Ectodomain Shedding of Transmembrane Carbonic Anhydrases

Fang-Ling Lin, Kui-Thong Tan, *et al.*

NOVEMBER 01, 2022  
ACS CHEMICAL BIOLOGY

READ 

### Predicting the Success of Fmoc-Based Peptide Synthesis

Ilanit Gutman, Bjoern Peters, *et al.*

JUNE 27, 2022  
ACS OMEGA

READ 

Get More Suggestions >